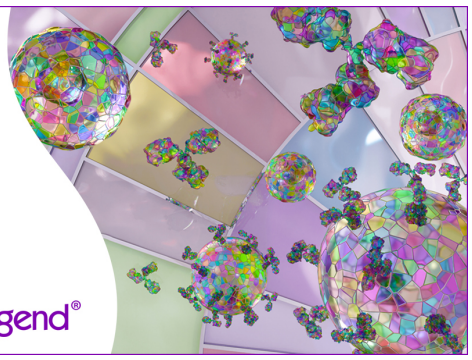

The Journal of Immunology
RESEARCH ARTICLE | NOVEMBER 15 2014

TCRs Genetically Linked to CD28 and CD3ε Do Not Mispair with Endogenous TCR Chains and Mediate Enhanced T Cell Persistence and Anti-Melanoma Activity FREE

Coen Govers; ... et. al

J Immunol (2014) 193 (10): 5315–5326.
https://doi.org/10.4049/jimmunol.1302074

TCRs Genetically Linked to CD28 and CD3ε Do Not Mispair with Endogenous TCR Chains and Mediate Enhanced T Cell Persistence and Anti-Melanoma Activity

Coen Govers,* Zsolt Sebestyén,* János Roszik,† Mandy van Brakel,* Cor Berrevoets,* Árpád Szöőr,† Konstantina Panoutsopoulou,* Marieke Broertjes,* Tan Van,* György Vereb,†,‡ János Szöllősi,†,‡ and Reno Debets*

Adoptive transfer of T cells that are gene engineered to express a defined TCR represents a feasible and promising therapy for patients with tumors. However, TCR gene therapy is hindered by the transient presence and effectiveness of transferred T cells, which are anticipated to be improved by adequate T cell costimulation. In this article, we report the identification and characterization of a novel two-chain TCR linked to CD28 and CD3ε (i.e., TCR:28ε). This modified TCR demonstrates enhanced binding of peptide–MHC and mediates enhanced T cell function following stimulation with peptide compared with wild-type TCR. Surface expression of TCR:28ε depends on the transmembrane domain of CD28, whereas T cell functions depend on the intracellular domains of both CD28 and CD3ε, with IL-2 production showing dependency on CD28:LCK binding. TCR:28ε, but not wild-type TCR, induces detectable immune synapses in primary human T cells, and such immune synapses show significantly enhanced accumulation of TCR transgenes and markers of early TCR signaling, such as phosphorylated LCK and ERK. Importantly, TCR:28ε does not show signs of off-target recognition, as evidenced by lack of TCR mispairing, as well as preserved specificity. Notably, when testing TCR:28ε in immune-competent mice, we observed a drastic increase in T cell survival, which was accompanied by regression of large melanomas with limited recurrence. Our data argue that TCR transgenes that contain CD28, and, thereby, may provide T cell costimulation in an immune-suppressive environment, represent candidate receptors to treat patients with tumors. ***The Journal of Immunology*****, 2014, 193: 5315–5326.**

Metastatic melanoma is a highly lethal disease with an incidence that continues to increase. Adoptive transfer of tumor infiltrating lymphocytes or TCR-engineered T cells showed clinical success in the treatment of metastatic melanoma (1, 2). For example, T cells expressing TCR transgenes that were directed against the HLA-A2–restricted Ags MART-1, gp100, or NY–ESO-1 mediated objective clinical responses in 12–45% of patients with metastatic melanoma (3, 4). Despite these significant antitumor responses, clinical studies are hindered by both toxicity and the transient nature of tumor regression in the majority of patients.

Treatment-related toxicity became evident from studies with TCRs, in particular those with high affinity directed against Ags that are overexpressed on tumors but also expressed (in some cases a highly similar Ag) on healthy cells. Toxicities included severe, but treatable, inflammation of skin, eyes, and ears (for MART-1/HLA-A2, gp100/HLA-A2) and colon (CEA/HLA-A2) (5, 6). In addition, lethal neurologic toxicities were observed in two melanoma patients when targeting MAGE-A3/HLA-A2, and lethal cardiac toxicities were observed in one melanoma patient and one multiple myeloma patient when targeting MAGE-A3/HLA-A1 (7, 8). The observed toxicities can be addressed by using TCRs directed against Ags that are selectively expressed by tumor but not healthy tissues, such as neoantigens and potentially some defined and nonshared cancer testis Ags (described in more detail in Ref. 1). In addition to the above-mentioned toxicities, TCR gene engineering may result in recognition of self-peptides as a consequence of new TCR dimers that are formed between introduced and endogenous TCR chains (i.e., TCR mispairing). Although there has been no formal proof of TCR mispairing–mediated toxicity in patient studies, preclinical studies clearly demonstrated the destructive ability of T cells that express mixed TCR dimers toward healthy cells (9, 10). These findings warrant measures to prevent or limit TCR mispairing, such as genetic modification of TCR transgenes (11) or disruption of endogenous TCR chains via zinc finger nucleases (12).

The transient nature of tumor regression following T cell therapy became evident from observations that antitumor responses are initially significant yet are not sustainable and most often are

*Laboratory of Tumor Immunology, Department of Medical Oncology, Erasmus University Medical Center Cancer Institute, 3015 CN Rotterdam, the Netherlands; †Department of Biophysics and Cell Biology, University of Debrecen, 4032 Debrecen, Hungary; and ‡Cell Biology and Signaling Research Group of the Hungarian Academy of Sciences, Medical and Health Science Center, University of Debrecen, 4032 Debrecen, Hungary

Received for publication August 6, 2013. Accepted for publication September 16, 2014.

This work was supported by European Union 6th Framework "Adoptive Engineered T cell Targeting to Activate Cancer Killing (ATTACK)" Grant 018914; National Science Foundation Theoretical Atomic, Molecular, and Optical Physics Grants TAMOP 4.2.1/B-09/1/KONV-2010-0007, TAMOP 4.2.2/B-10/1/2010-0024, and TAMOP 4.2.2/A-11/1/KONV-20120025; Hungarian Scientific Research Fund Grant OTKA NK 101337; and Baross Gabor Program Grant REG_EA_09-12009-0010.

Address correspondence and reprint requests to Dr. Reno Debets, Laboratory of Tumor Immunology, Department of Medical Oncology, Erasmus University Medical Center Cancer Institute, Wytemaweg 80, 3015 CN Rotterdam, the Netherlands. E-mail address: j.debets@erasmusmc.nl

The online version of this article contains supplemental material.

Abbreviations used in this article: APL, altered peptide ligand; CAR, chimeric Ag receptor; FRET, fluorescence resonance energy transfer; gp100/A2, $gp100_{280–288}$/HLA-A*0201; IC, intracellular; INF, influenza; M1/A1, $MAGE\text{-}A1_{161–169}$/HLA-A*0101; MFI, mean fluorescence intensity; O/N, overnight; TCR:28ε, TCR genetically linked to CD28 and CD3ε; tg, transgenic; TM, transmembrane; wt, wild-type.

incomplete in 80–90% of patients (13, 14). Compromised antitumor responses often coincided with a limited persistence of transferred T cells (15). T cell persistence and antitumor activity appear sensitive to T cell costimulation, as pointed out by a recent clinical study in which T cells engineered with a CD19-specific chimeric Ag receptor (CAR) that incorporated CD137 and CD3ζ were used to treat patients with B cell lymphoma. In this study, T cell persistence was significant (detectable up to 6 mo); complete clinical responses were initially observed in two of three patients (16) and subsequently confirmed in dozens of patients (17). Similarly, clinical studies using CD19-targeted T cells with CARs that incorporated CD28 and CD3ζ showed beneficial effects on long-term T cell persistence and clinical responses (18, 19). In addition to genetic engineering, MART-1–specific T cells stimulated with artificial APCs that expressed CD28 ligands and used to treat patients with melanoma revealed enhanced T cell persistence and clinical responses (20). Importantly, inclusion of T cell costimulation in these clinical protocols eliminated the requirement for patient preconditioning with chemotherapy and/or in vivo high-dose IL-2 administration (16, 20).

In this study, we designed and generated a novel TCR genetically linked to CD28 and CD3ε (TCR:28ε) to simultaneously address TCR mispairing and enhance T cell costimulation. TCR:28ε was tested for two melanoma Ag specificities, MAGE-A1/HLA-A1 and gp100/HLA-A2, and resulted in maximum ability to bind peptide–MHC, enhanced peptide responses, no TCR mispairing, and no loss of Ag or peptide fine specificity. Moreover, T cells expressing TCR:28ε mediated highly active immune synapses and early T cell signaling and resulted in improved T cell survival and reduced numbers of melanoma recurrences in vivo.

Materials and Methods

Cells and reagents

T lymphocytes derived from healthy donors were isolated and expanded using a feeder system, as described elsewhere (21), and cultured in HEPES-buffered RPMI 1640 medium (BioWhittaker, Verviers, Belgium) supplemented with 10% human serum (Sanquin, Amsterdam, the Netherlands), 2 mM L-glutamine, 100 μg/ml streptomycin, and 100 U/ml penicillin. Jurkat T cells expressing a single MelanA/HLA-A2–specific TCR [clone J.19 (22)], J.19 transduced with CD8α [J.19-CD8 (23)], the B cell lines APD and BSM, and the TAP-deficient TxB hybrid T2 cells were cultured in RPMI 1640 medium (BioWhittaker) containing 10% FBS (Stonehouse, Gloucestershire, U.K.) and antibiotics. The packaging cell lines 293T and Phoenix-A and the melanoma cell lines G43, MZ2-MEL43, GE-F-, FM3, and Mel2A were cultured in DMEM (BioWhittaker) containing 10% FBS, 2 mM L-glutamine, nonessential amino acids, and antibiotics. Abs used in this study were PE-conjugated TCR-Vβ9 (clone BL37.2 for flow cytometry and clone IM2355 for microscopy; Beckman Coulter, Marseille, France), nonconjugated and FITC-conjugated TCR-Vα19 (clone 6D6.6; Pierce Biotechnology, Rockford, IL), PE-conjugated TCR-Vβ27 (clone CAS1.1.3; Beckman Coulter), nonconjugated CD3ε (clone OKT3; Beckman Coulter), PerCP-conjugated CD3ε (clone SP34-2; BD Biosciences, San Jose, CA), nonconjugated CD8α (clone UCHT4; Adipogen, San Diego, CA), PE-conjugated CD107a (clone H4A3; BD Biosciences), Alexa Fluor 647–conjugated p-CD3ζ (SC-9975; Santa Cruz Biotechnology, Heidelberg, Germany), p-LCK (clone SC-28445-R; Santa Cruz Biotechnology), p-ERK (clone SC-7976; Santa Cruz Biotechnology), p-ZAP70 (clone SC-33526; Santa Cruz Biotechnology), Cy5-conjugated RαM (Jackson ImmunoResearch, West Grove, PA), and Alexa Fluor 647–conjugated GαM (Life Technologies-Invitrogen, Paisley, U.K.). Alexa Fluor 647–conjugated CD3ε, CD8α, and CD45 Abs were acquired and conjugated as described previously (23). MAGE-A1$_{161–169}$/HLA-A*0101 (M1/A1) and gp100$_{280–288}$/HLA-A*0201 (gp100/A2) tetramers were generated from biotinylated monomers (Sanquin) and streptavidin-PE (BD Biosciences) (24). Other reagents used in this study included retronectin (human fibronectin fragments CH-296; Takara Shuzo, Otsu, Japan), PMA (Sigma-Aldrich, St. Louis, MO), PHA (Remel Europe, Dartford, U.K.), GolgiStop (BD Biosciences), influenza (INF) peptide (CTELKLSDY), M1 peptide (EADPTGHSY), and gp100 peptide (YLEPGPVTA) (ProImmune). Altered peptide ligands of gp100 peptide (A1–A8 and G9) were synthesized as described previously (25).

TCR gene constructs

The M1/A1 TCR was derived from CTL clone MZ2-82/30 (26, 27) and is composed of TRAV19/J39/C and TRBV9/D2/J2-3/C2; the gp100/A2 TCR was derived from CTL clone 296 and is composed of TRAV13-1/J52/C and TRBV27/J2-7/D2/C2 (25) [with TCR-V(D)J gene nomenclature according to http://www.imgt.org]. The 28ε cassette was derived via overlap PCR using human PBMC-derived template DNAs and covered the transmembrane (TM) and intracellular (IC) domains of human CD28 (GI: 338444, aa 153–220, numbering starting from first methionine), followed by the IC domain of human CD3ε (GI:4502670, aa 153–207). The 28ε cassette was preceded by the amino acids GSPK (with GS covering a BamHI site) and cloned into both pBullet-TCRα (TCR-Cα amino acids ending at SPESS) and TCRβ (TCR-Cβ amino acids ending at WGRAD) via NotI and BamHI. Primer sequences used for cloning the TCR and 28ε cassette can be provided upon request. All TCR constructs were sequence verified (Service XS, Leiden, the Netherlands). See Fig. 1A for a schematic representation of the two-chain TCR:28ε. TCR variants in which TM or IC domains were replaced, deleted, or mutated were generated by overlap PCR. See Fig. 3A for a schematic overview of these TCR variants and its legend for the exact domain boundaries. TCR variants included TCR:TMζ-IC28ε (CD3ζ TM; described in Ref. 27), TCR:TM28-ICε (CD28 IC domain removed), TCR:TM28-IC28ζ (TCR:28ζ; described in Ref. 28), and TCR:TM28-IC28(mut)ε [CD28 IC domain mutated to prevent LCK binding, as described (29)].

Retroviral gene transfer into T cells

Moloney murine leukemia retroviruses were produced by cocultures of 293T and Phoenix-A cells. Cells were calcium phosphate transfected with TCR transgenes, the helper vectors pHIT60 MLV GAG/POL, and either pVSV-G ENV or pCOLT-GALV ENV in the case of Jurkat T cells or primary human T cells, respectively. The transduction protocol of human T cells was optimized and described previously (30).

Flow cytometry and FACS

TCR-transduced T cells were washed and incubated with TCR mAbs or peptide–MHC for 30 min on ice or 15 min at room temperature, respectively, after which T cells were washed again and fixed with 1% PFA (Brunschwig, Amsterdam, the Netherlands). To detect CD107a mobilization, T cells were stimulated with target cells and analyzed as described (31). T cells were gated according to forward and side scatter properties using a FACSCalibur (Becton Dickinson, Alphen a/d Rijn, the Netherlands) equipped with CellQuest software (BD Biosciences). Enrichment of T cells was performed by two-color FACS following staining with TCR-α and TCR-β mAbs (for M1/A1) or peptide–MHC (for gp100/A2).

T cell assays

T cell IFN-γ and IL-2 production was determined as described previously (28). In short, T cells were stimulated with APD or BSM B cells loaded or not with peptides or melanoma cell lines, and overnight (O/N) supernatants were collected and tested for the presence of cytokines by ELISAs. The NFAT reporter gene assay was performed as described previously (31). Briefly, Jurkat clone J.19 cells (5×10^6) were nucleofected with 5 μg firefly luciferase reporter gene encompassing six response elements of the NFAT-6–Luc using Amaxa's nucleofector and program C-16, according to the manufacturer's protocol (Amaxa Biosystems, Cologne, Germany). Next, T cells were transferred to prewarmed medium and incubated O/N at 37°C with 5% CO_2. Nontissue culture–treated 96-well plates were coated O/N at 4°C with anti–TCR-Vβ9, anti–TCR-Vβ27, or nonconjugated control mAb. T cells (0.2×10^6) were incubated in precoated 96-well plates for 6 h at 37°C with 5% CO_2, and lysates (Cell Lysis Buffer; Promega, Madison, WI) were collected and used to measure photon emissions in a luminometer (Mediators, Vienna, Austria) using luminescent substrates, according to the manufacturer's instructions. Results are expressed as relative luminescence units relative to nonstimulated controls (medium only was set at 1.0).

Microscopic and flow cytometric fluorescence resonance energy transfer

TCR-transduced Jurkat clone 19 T cells and primary human T cells were prepared for confocal microscopy as described previously (23). Target APD B cells were loaded with 10^{-5} M M1 or INF peptide and subsequently labeled with 5 μM CFSE (Life Technologies-Invitrogen). T cells and target cells were

fixed and stained with TCR–Vβ9–PE mAb and one of the following mAbs (labeled with Alexa Fluor 647 or followed by GαM–Alexa Fluor 647)— CD3ε, CD8α, CD45, p-CD3ζ, p-LCK, p-ERK, or p-ZAP70— covered with glycerol:PBS, and analyzed with a confocal microscope (LSM 510; Carl Zeiss, Jena, Germany). Data were collected using ImageJ software (National Institutes of Health, Bethesda, MD). Confocal images were taken in the donor, acceptor, and CFSE channels (the last channel for target cells) prior to and postphotobleaching. Fluorescence resonance energy transfer (FRET) efficiencies/pixel were calculated using the AccPbFRET program (32). The relative density of synaptic molecules was calculated as the ratio of mean fluorescence intensities (MFIs)/pixel inside versus outside the immune synapse. TCR-transduced Jurkat clone 19 T cells also were subjected to flow cytometric FRET. To this end, T cells were stained with TCR–Vβ9–PE or TCR–Vβ27–PE mAbs to provide donor fluorochromes and with nonconjugated TCR-Vα19, CD3ε, or CD8α mAbs, followed by RαM-Cy5 mAb, to provide acceptor fluorochromes, as described previously (22). Fluorescence intensities of donor, acceptor, and FRET signals were measured and collected on a FACSCalibur. Data for viable T cells were analyzed with Reflex software on a per-cell basis (33).

Mice

Experiments were performed with HLA-A2–transgenic (tg) mice (kindly provided by Prof. François Lemonnier, Institut Pasteur, Paris, France and described in Ref. 34), in accordance with institutional and national guidelines, following approval by the Experimental Animal Committee of the Erasmus University Medical Center Cancer Institute.

Generation of mouse TCR T cells and human gp100/A2$^+$ B16 melanoma cells

gp100/A2-specific TCR genes were murinized (35), codon optimized (GeneArt, Regensburg, Germany), and cloned into the pMP71 vector (kindly provided by Prof. Wolfgang Uckert, Max-Delbrück Center, Berlin, Germany). TCRα and TCRβ genes were separated by an optimized T2A ribosome-skipping sequence, resulting in pMP71:wild type (wt)TCRβ–T2A–wtTCRα. gp100/A2-specific murinized TCR:28ε genes were made by overlap PCR and insertion of a 28ε cassette (murine, codon-optimized) in pMP71:wtTCRβ–T2A–wtTCRα (NcoI/MfeI flanking TCRβ; MluI/EcoRI flanking TCRα). The murine 28ε cassette was synthesized in exact analogy to its human counterpart (TM+IC GSPK-CD28$_{151–218}$ [GI:39850201]; IC CD3ε$_{135–189}$ [GI:289655610]). The Ag gene (gp100/A2) was obtained by inserting DNA that covered the leader sequence of HLA-A2, the gp100 peptide YLEPGPVTA, and a $(G_4S)_3$ linker and was cloned via EcoRI into a pLXSN vector that already contained HHD. HHD cDNA was subcloned as an XhoI fragment into the retroviral vector pLXSN (Clontech Laboratories, Mountain View, CA).

Total mouse splenocytes were isolated, activated with Con A and recombinant human IL-2, and transduced with the retroviral supernatant containing TCR RNAs, as described by Pouw et al. (35). B16 cells were retrovirally transduced using a similar transduction protocol, with the exception that GALV-pseudotyped viruses and Polybrene (4 μg/ml) were used, and cells were incubated with the retroviral supernatant for 24 h, followed by a second incubation for 8 h. B16:gp200/A2 cells were single-cell sorted for high HLA-A2–expressing cells on a FACSAria cell sorter using the anti–HLA-A2 Ab and cultured under neomycin selection. TCR surface expression, binding of peptide-MHC, and in vitro T cell functions were assessed as described in Supplemental Fig. 3.

Adoptive T cell therapy

For adoptive T cell therapy experiments, HLA-A2–tg mice were injected s.c. with 0.5×10^6 B16:gp100/A2 cells, and 10 and 11 d later, they received a total of two busulphan (Duchefa Farma, Haarlem, the Netherlands) injections i.p. (16.5 μg/kg each), followed 1 d later by a single i.p. injection (200 mg/kg) of cyclophosphamide (Sigma-Aldrich). Mice received 7.5×10^6 murinized wt TCR or TCR:28ε T cells at day 13. Tumor growth was measured using a caliper three times a week, and tumor volumes were estimated as described (36). Peripheral blood was drawn at days 12, 26, and 40 after T cell transfer. TCR-transduced T cells were monitored with anti–TCR-Vβ27 mAb (nomenclature according to http://www.imgt.org; clone CAS1.1.3, Beckman Coulter) and gp100/A2K^b PE-labeled peptide–MHC [gp100/A2 peptide–MHC generated as described (37)] in combination with PerCP-labeled anti-CD3ε and allophycocyanin-labeled anti-CD8a mAbs using standard flow cytometry. Absolute T cell counts were determined using Flow-Count Fluorospheres. All samples were analyzed on a FACSCalibur using CellQuest software (BD Biosciences).

Statistical analysis

Statistically significant differences between TCR:28ε and wt TCR were tested by nonpaired and two-tailed Student *t* tests using GraphPad Prism4 software. Differences with p values < 0.05 were considered significant.

Results

A signaling cassette consisting of CD28 and CD3ε results in improved surface expression and function of TCRαβ-chains

We initially selected signaling cassettes that consisted of Fc(ε)RI, CD3ε, and CD3ζ accessory molecules, with or without the CD28 costimulatory molecule, according to their effect on the functional expression of single-chain TCR transgenes (Z. Sebestyen, M. Broertjes, C. Govers, M. van Brakel, and R. Debets, manuscript in preparation). These data argued that the CD28-CD3ε (28ε) signaling cassette consistently provided T cells with the best binding of peptide–MHC, T cell cytotoxicity, and IFN-γ. We introduced the 28ε cassette into a two-chain TCR format (i.e., TCR:28ε; Fig. 1A), gene transduced primary human T cells with M1/A1 wt TCR or TCR:28ε, and used FACSort to obtain T cell populations with high and equal levels of TCR expression (>95%) (Fig. 1B). Following staining with TCRα and TCRβ mAbs, flow cytometry dot plots of TCR:28ε$^+$ T cells revealed a typical diagonal with enhanced MFI values and equal staining intensities for TCRα− and TCRβ-chains. This staining pattern suggests correct pairing of TCRα and TCRβ transgenes and was similar to the pattern reported previously for TCR:ζ (22, 31). Following staining with peptide–MHC, TCR:28ε T cells demonstrated a significantly enhanced percentage and MFI over a range of peptide–MHC concentrations compared with wt TCR T cells (Fig. 1B, 1C).

To investigate T cell function, we stimulated TCR-engineered T cells with anti-TCR Abs, peptide-loaded cells, and native melanoma cells and analyzed activation of NFAT, mobilization of CD107a, and production of cytokines. Using a luciferase reporter assay with Jurkat T cells, we observed a significantly greater activation of NFAT upon stimulation of TCR:28ε T cells with TCR-Vβ9 Ab (against the introduced M1/A1 TCR) compared with wt TCR T cells (Fig. 2A). T cells transduced with wt TCR, but not with TCR:28ε, demonstrated decreased NFAT activation upon stimulation with TCR-Vβ27 Ab (against the endogenous MelanA/A2 TCR). These findings suggest that enhanced functional expression of TCR:28ε does not occur at the expense of the functional expression of endogenous TCR. When assessing CD107a mobilization in primary human T cells, we observed that TCR:28ε showed enhanced performance upon stimulation with M1 peptide and equal performance upon stimulation with native, M1/A1$^+$ melanoma cells compared with wt TCR (Fig. 2B). Using TCRs directed against a second Ag (i.e., gp100/HLA-A2 [gp100/A2]), we confirmed enhanced peptide–MHC binding (Supplemental Fig. 1A) and peptide-induced mobilization of CD107a by TCR:28ε (Fig. 2C). Enhanced responsiveness toward peptide-loaded targets cells of both M1/A1- and gp100/A2-specific TCRs also was observed upon assessing TCR:28ε T cells for their production of IFN-γ and IL-2 (see figure below and Supplemental Fig. 1B, 1C).

The CD28 TM domain determines surface expression of TCR:28ε, and both CD28 and CD3ε IC domains determine T cell functions

We generated and tested new TCR variants in vitro to discern the contributions of the TM and IC domains of CD28 and CD3ε to the above-mentioned TCR properties. A schematic representation of the TCR variants is given in Fig. 3A. We observed that the TCR variant not having the CD28 TM domain (TCR:TMζ-IC28ε) did

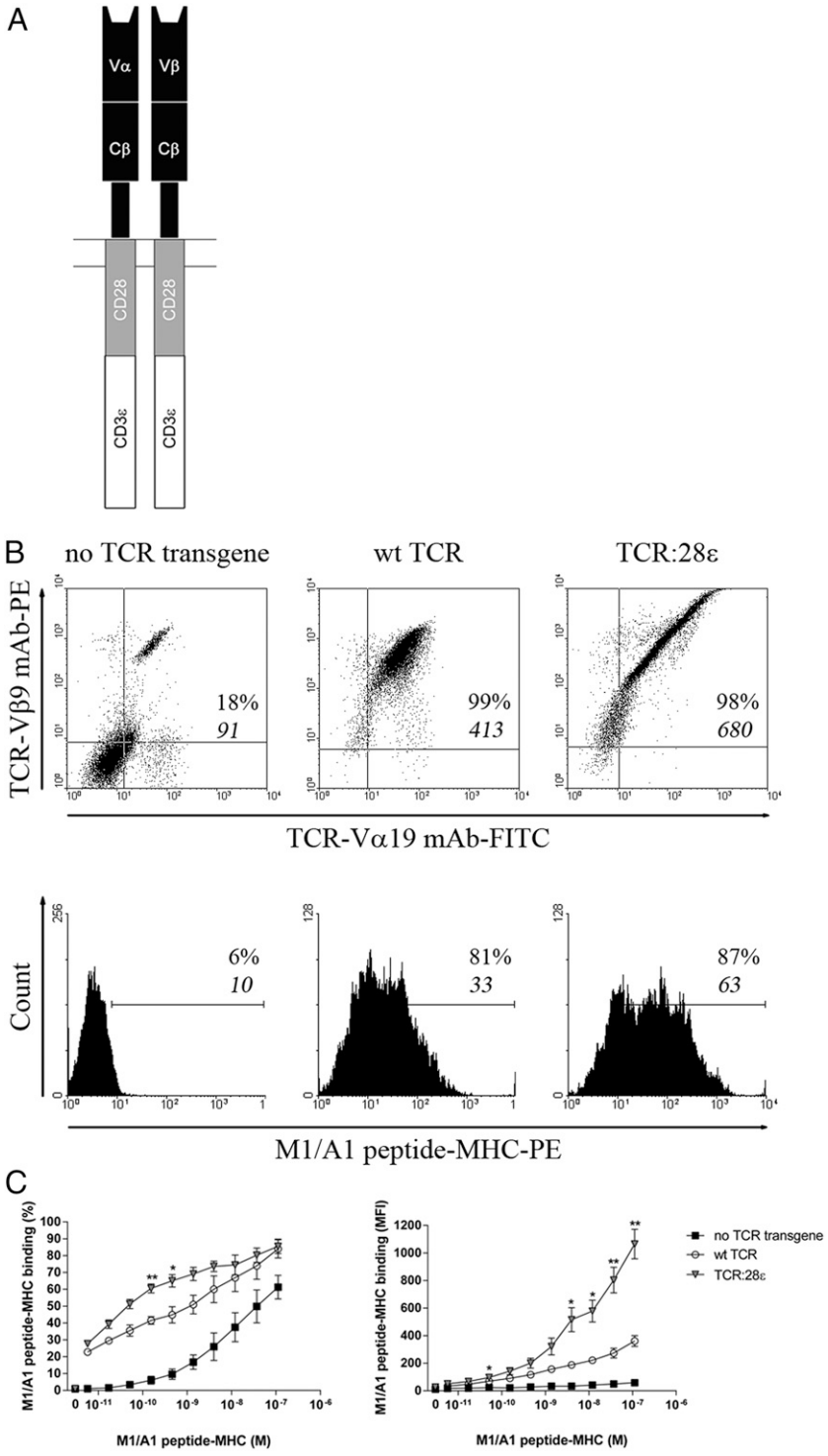

FIGURE 1. TCR:28ε shows enhanced peptide–MHC binding. Primary human T cells were transduced with empty virus particles (no TCR transgene), M1/A1 TCR (wt TCR), or TCR:28ε. (**A**) Schematic representation of TCR:28ε. See *Materials and Methods* for details on the 28ε-signaling cassette. (**B**) T cells were sorted by FACS with TCR-Vα19 and TCR-Vβ9 mAbs and analyzed by flow cytometry following staining with mAbs directed against TCRα and TCRβ (*upper panels*) or M1/A1 peptide–MHC (*lower panels*). Dot plots and graphs represent measurements of PBMCs (n = 3) from two healthy donors with similar results. For dot plots, percentages correspond to the *upper two quadrants*, and MFIs (in italics) correspond to the x-axes of the *upper right quadrants*. For graphs, percentages and MFI correspond to marker-positive cells. Nonstained T cells were used to gate viable cells and set ordinates and markers at <1% T cells. (**C**) T cells were stained with titrated amounts of M1/A1 peptide–MHC (10^{-11} to 10^{-7} M), and results are expressed as percentage (*left panel*) or MFI (*right panel*) (n = 3 independent measurements). $*p < 0.05$, $**p < 0.005$ TCR:28ε versus wt TCR, Student t test.

not express on the cell surface (Fig. 3A), whereas the TCRs not having CD28 or CD3ε IC domains or having a mutated CD28 IC domain [TCR:TM28-ICε, TCR:TM28-IC28ζ, and TCR:TM28-IC28(mut)ε] exhibited unaltered peptide–MHC binding compared with the parental TCR:28ε (Fig. 3B). These data suggest that the CD28 TM domain is of critical importance for the enhanced surface expression and peptide–MHC binding that was observed for TCR:28ε (Fig. 1B, 1C). Furthermore, we observed that TCRs lacking the CD28 or CD3ε IC domains mediated decreased CD107a mobilization and IFN-γ and IL-2 production in response to peptide (Fig. 3C–E). When the CD3ε IC domain was replaced by the CD3ζ IC domain (TCR:TM28-IC28ζ), all three T cell readouts were markedly decreased (~75% decrease compared with TCR:28ε). Interestingly, in the absence of the CD28 IC domain (TCR:TM28-ICε), the decrease in T cell CD107a mobilization was limited (~25%), the decrease in IFN-γ production was substantial (~50%), and the decrease in IL-2 production was most pronounced (~75%). The CD28 IC domain shows two main motifs, each with characteristic binding partners and downstream signal transduction (a simplified version of CD28 IC domain is presented in Fig. 3A). The testing of TCR:TM28-IC28(mut)ε, containing a mutated PYAPP motif and not able to bind LCK (Fig. 3A), revealed that the increased requirement for CD28 signaling with respect to

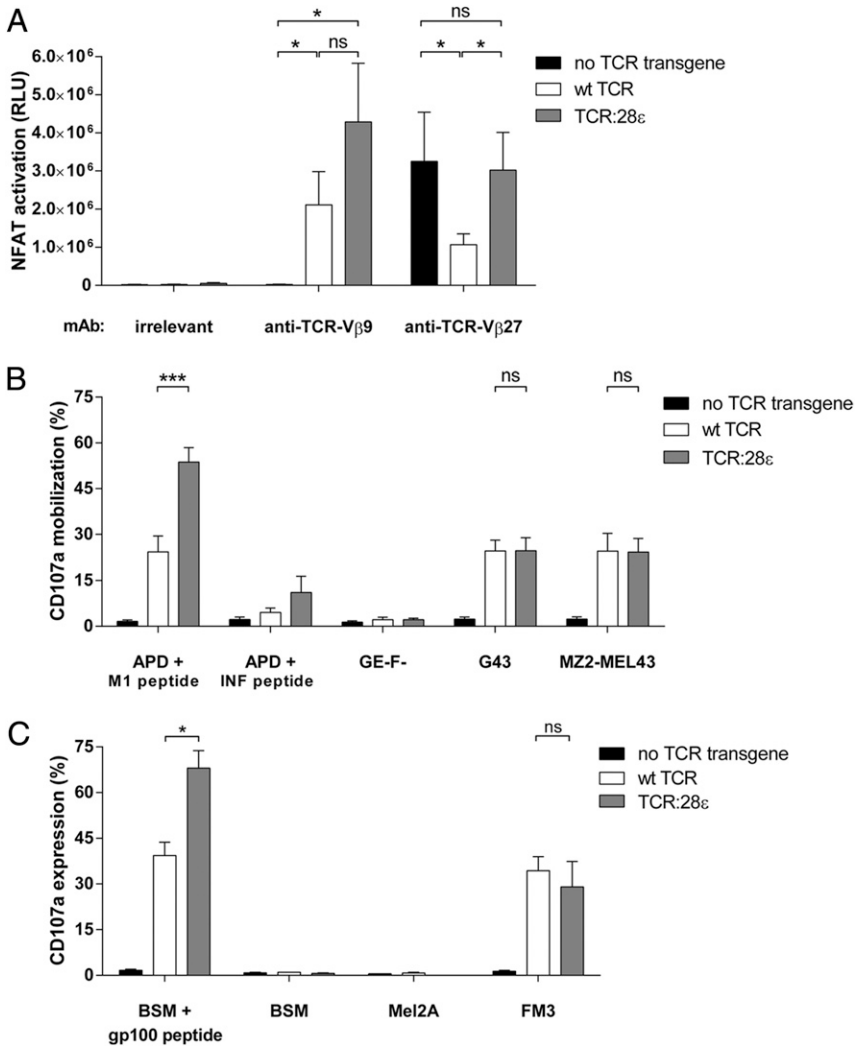

FIGURE 2. TCR:28ε T cells demonstrate enhanced activation of NFAT and Ag-specific mobilization of CD107a. Jurkat clone 19 T cells (**A**) and primary human T cells (**B** and **C**) were transduced with empty virus particles, M1/A1 or gp100/A2 wt TCR, or TCR:28ε; sorted by FACS with TCRα and TCRβ mAbs (for M1/A1) or peptide–MHC (for gp100/A2); and tested for their ability to mediate activation of NFAT (A) or mobilize CD107a to the cell surface upon stimulation with Ag (B and C). (A) M1/A1 TCR Jurkat T cells were nucleofected with a firefly luciferase reporter construct under control of NFAT response elements and stimulated for 6 h with irrelevant, anti–TCR-Vβ9 or anti–TCR-Vβ27 mAb coated to well plates. Bars represent mean activation of NFAT expressed in relative luminescence units (RLU) + SEM (n = 5 independent measurements). Mock T cells showed negligible levels of NFAT activation (data not shown). (B) M1/A1 TCR T cells were stimulated with the APD B cell line ($A1^+$) loaded with M1 or INF peptide ($10\ M^{-5}$ final) and the melanoma cell lines GE-F- ($M1^-/A1^+$), G43, and MZ2-MEL43 (both $M1^+/A1^+$). (C) gp100/A2 TCR T cells were stimulated with the BSM B cell line ($A2^+$) loaded or not with gp100 peptide ($10\ M^{-5}$ final) and the melanoma cell lines FM3 ($gp100^+/A2^+$) and Mel2A ($gp100^+/A2^-$). CD107a mobilization was measured by flow cytometry and expressed as the percentage of $CD107a^+$ cells within the population of $CD3^+$ cells. Bars represent mean + SEM (n = 2–10 independent measurements). $*p < 0.05$, $***p < 0.0005$ TCR:28ε versus wt TCR, Student t test. ns, nonsignificant.

CD107a mobilization and IFN-γ and IL-2 production was accompanied by an increased requirement for LCK-mediated signaling (decreases were approximately 0% for CD107a, 25% for IFN-γ, and 50% for IL-2) (Fig. 3C–E).

TCR:28ε induces immune synapses with enhanced accumulation of TCR, CD3ε, and CD8α and phosphorylated LCK and ERK

The induction of immune synapses and their molecular profile are considered a critical measure of T cell activation. To study the induction ability and the composition of immune synapses, TCR-transduced Jurkat T cells were stimulated with M1 peptide–loaded target cells and analyzed by confocal microscopic FRET. We observed that TCR:28ε is able to induce immune synapses, and TCR:28ε present in immune synapses does not associate with CD3ε but does associate with CD8α (Supplemental Fig. 2A, 2B). In addition, the immune synapses induced by TCR:28ε and wt TCR are of similar size (Supplemental Fig. 2C). Notably, when repeating analyses with TCR-engineered primary human T cells, TCR:28ε, but not wt TCR, mediated detectable Ag-induced immune synapse formation (Fig. 4A, 4B). To investigate synaptic accumulation of T cell membrane molecules in more detail, we used quantitative analysis of confocal microscopy data and observed that TCR:28ε mediated a 5-fold increase in the accumulation of TCRβ transgene and endogenous CD3ε and CD8α molecules compared with wt TCR (Fig. 5A). When measuring markers of early T cell activation, we noted that TCR:28ε mediated the accumulation of p-LCK (7-fold increase) and, to a lesser extent, p-ERK (~2-fold increase) (Fig. 5B). However, TCR:28ε mediated a significantly decreased accumulation of p-CD3ζ (~ 2-fold) but did not affect the accumulation of p-ZAP70 (Fig. 5B).

TCR:28ε does not appear sensitive to off-target recognition in vitro

To assess whether TCR:28ε is prone to off-target recognition, we performed two types of in vitro assays. First, we performed flow cytometric FRET to determine the extent of mispairing between introduced TCR:28ε and endogenous (wt) TCR chains. To this end, we transduced a Jurkat T cell clone already expressing the MelanA/A2 wt TCR and the CD8α coreceptor with the M1/A1 wt TCR or TCR:28ε gene. Measurements of flow cytometric FRET using MelanA/A2 TCR-Vβ27–specific and M1/A1 TCR-Vα19–specific mAbs revealed significant energy transfer in the case of wt TCR but not TCR:28ε (values were <5% background signal) (Fig. 6A). Measurements of FRET using the M1/A1 TCR-Vβ9 and either CD3ε or CD8α mAb showed that TCR:CD3 associations were observed for wt TCR but not TCR:28ε, whereas TCR:CD8α associations were present for both TCR formats (Fig. 6A). Observations with flow cytometric FRET extend earlier observations with microscopic FRET using primary human T cells or Jurkat T cells (Fig. 4B and Supplemental Fig. 2B). These experiments show that TCR:28ε does not mispair with endogenous TCR chains

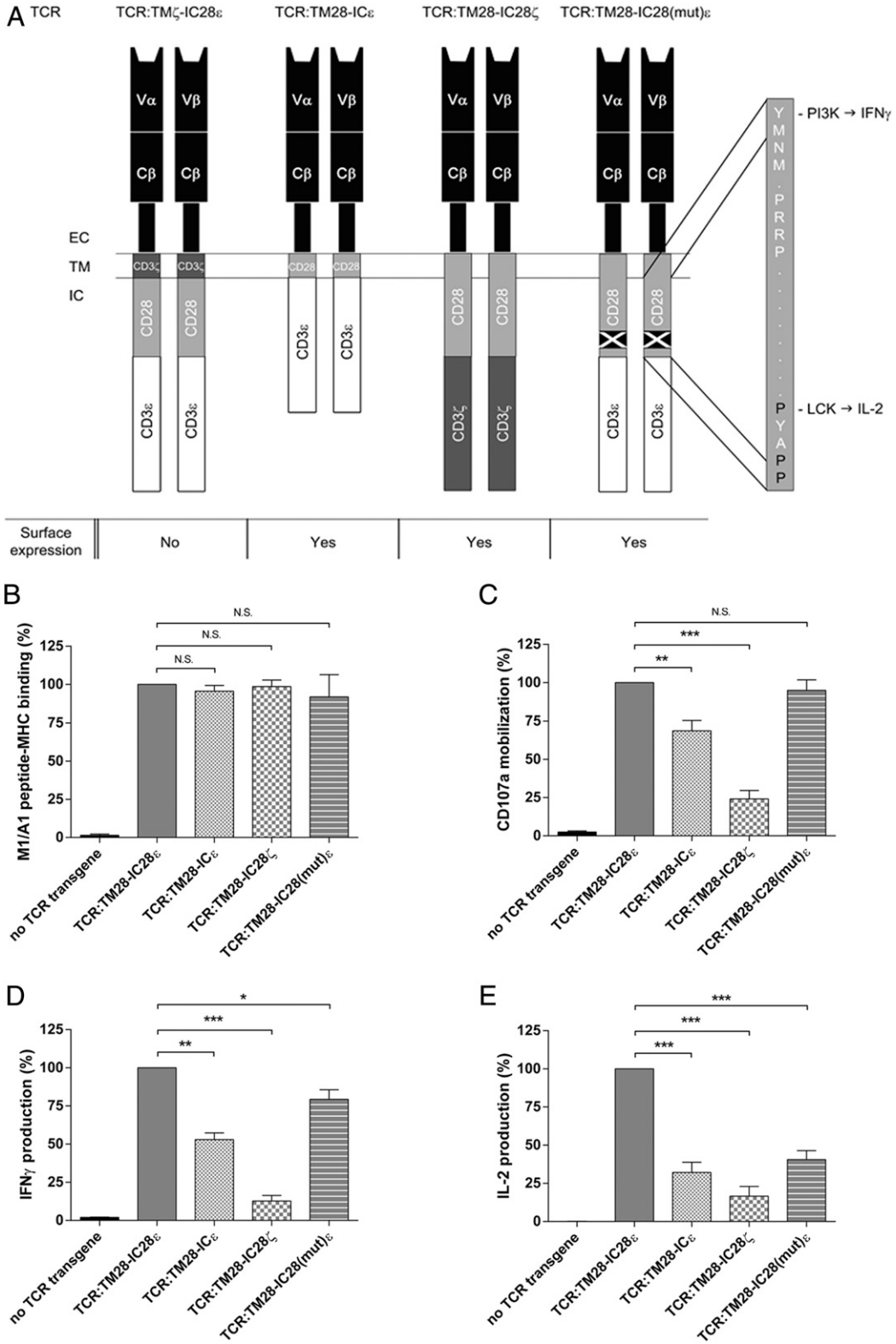

FIGURE 3. Surface expression of TCR:28ε depends on TM domain of CD28, and T cell functions depend on IC domains of both CD28 and CD3ε. Primary human T cells were transduced with empty virus particles (no TCR transgene) or one of the following M1/A1 TCR variants: TCR:TM28-IC28ε (TCR:28ε), TCR:TMζ-IC28ε, TCR:TM28-ICε, TCR:TM28-IC28ζ (TCR:28ζ), or TCR:TM28-IC28(mut)ε. (**A**) Schematic representation of TCR variants, together with an illustration of CD28 IC amino acids. The CD28 IC domain shows two main motifs, each with characteristic binding partners and downstream signal transduction (for simplicity reasons only limited binding partners and signal transduction have been displayed, see text for details). Amino acids of the PYAPP motif that are mutated to prevent LCK binding are in black. All TCR variants are derived from TCR:28ε, and the amino acid boundaries of domains are as follows: TM $CD28_{153–179}$ (GI:338444) is replaced by TM $CD3\zeta_{31–51}$ (GI:4557430); IC $CD28_{180–220}$ is removed or mutated at P208A, P210A, and P211A; and IC $CD3\varepsilon_{153–207}$ (GI:4502670) is replaced by IC $CD3\zeta_{52–164}$. T cells were sorted by FACS with TCRα and TCRβ mAbs and analyzed by flow cytometry for M1/A1 peptide–MHC binding (**B**) or CD107a mobilization (**C**) or by ELISA for IFN-γ (**D**) or IL-2 (**E**) production. Assays and analyses were performed as described in Figs. 1 and 2. Bars represent measurements of PBMC (n = 3–5), and results with TCR:28ε were set to 100%. *$p < 0.05$, **$p < 0.005$, ***$p < 0.0005$ TCR:28ε versus wt TCR, Student t test. EC, extracellular; IC, intracellular; N.S., nonsignificant; TM, transmembrane.

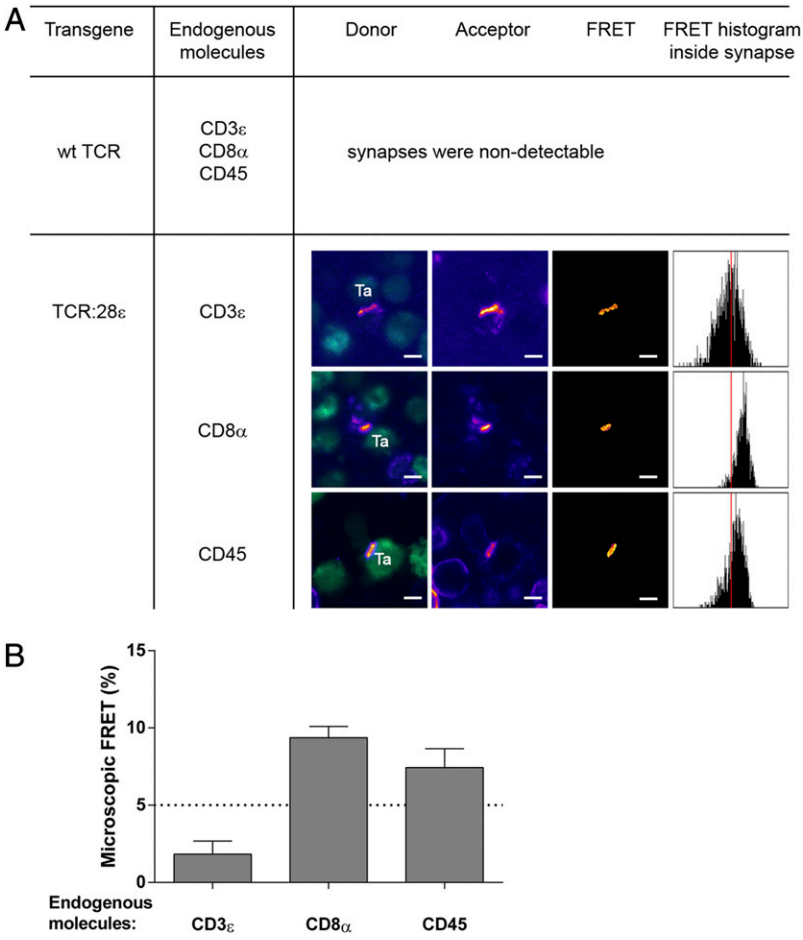

FIGURE 4. TCR:28ε, but not wt TCR, induces formation of Ag-dependent immune synapses in primary human T cells. Primary human T cells were transduced with M1/A1 wt TCR or TCR:28, as described in Fig. 1, and analyzed for molecular associations between the TCRβ transgene and endogenous CD3ε, CD8α, or CD45 molecules in immune synapses. APD B cells (marked as target cells; Ta) were stained with CFSE, loaded with M1 peptide, and used to stimulate TCR T cells. T cells were labeled with TCR–Vβ9–PE mAb and one of the following Alexa Fluor 647–labeled mAbs—CD3ε, CD8α, or CD45—and confocal microscopy was used to measure FRET. (**A**) Representative photomicrographs of immune synapses of primary human T cells (original magnification ×200; scale bars, 5 μm), including FRET graphs of corresponding immune synapses. Vertical red lines in the center of graphs denote zero FRET efficiency/pixel in the synapse region. TCR T cells stimulated with APD B cells loaded with irrelevant peptide showed low background levels of FRET (except for FRET between wt TCR and CD3ε) (data not shown). (**B**) Mean percentage + SEM of microscopic FRET measured with primary human T cells (n = 3 independent measurements of 15 cells/measurement). The dotted line represents a 5% background signal below which no distinction between significant and nonsignificant interactions can be made.

nor does it associate with endogenous CD3 molecules, similar to observations reported for a TCR that is fused to a complete CD3ζ molecule (i.e., TCR:ζ) (22, 31). Second, we assessed T cell function in response to gp100 altered peptide ligands (APLs) to determine the extent to which peptide fine specificity of TCR:28ε is changed compared with wt TCR. To this end, we loaded T2 cells with gp100 APL, as described by Schaft et al. (25), and measured IFN-γ production following stimulation of TCR-transduced primary human T cells. We observed that both TCR:28ε and wt TCR mediated IFN-γ production to all APLs, except when alanine replaced glutamic acid at position 3 (Fig. 6B). This peptide response pattern was identical to that of the parental CTL-296 clone (25) and showed that incorporation of the 28ε cassette did not alter the peptide fine specificity of the parental TCR.

Mouse T cells expressing TCR:28ε limit and delay tumor recurrence and demonstrate enhanced peripheral T cell persistence

Finally, we set out to assess the in vivo behavior of T cells transduced with TCR:28ε. To this end, we constructed murinized gp100/A2-specific wt TCR and TCR:28ε (see *Materials and Methods*) and retrovirally transduced them into mouse splenocytes. Mouse T cells transduced with TCR:28ε showed enhanced surface expression and were able to kill gp100/A2$^+$ B16 melanoma cells (Supplemental Fig. 3). For adoptive T cell therapy studies, HLA-A2–tg mice were transplanted with B16:gp100/A2 tumor cells; once tumors were palpable (in some cases >500 mm^3), mice were conditioned with busulphan and cyclophosphamide and treated with 7.5 × 10^6 T cells transduced either with TCR:28ε or wt TCR. Notably, T cells expressing TCR:28ε effectively limited tumor recurrence, because 4 out of 8 mice were tumor-free, whereas none of the mice treated with wt TCR T cells were tumor-free at 40 d posttreatment (Fig. 7A). Also, the day on which tumors recurred following treatment was significantly delayed in the case of TCR:28ε (Fig. 7C, day 35 versus 18). The effect on tumor recurrence was accompanied by a drastic increase in the numbers of peripheral CD8 T cells that bound peptide–MHC (in some cases >1500/μl blood) and remained stable until the end of the experiment (6 wk after treatment, Fig. 7B, 7D).

Discussion

In this study, we designed and generated a novel TCR genetically linked to CD28 and CD3ε (TCR:28ε). TCR:28ε was tested for two melanoma Ag specificities and provided T cells with the following beneficial properties for T cell therapy: enhanced peptide–MHC binding, more potent T cell responses upon stimulation with peptide and equal responses upon stimulation with Ag$^+$ melanoma cells, formation of highly active immune synapses, no TCR mispairing and no change in peptide fine specificity, and improved T cell survival and reduced numbers of melanoma recurrences in vivo.

The enhanced ability of T cells transduced with TCR:28ε to bind peptide–MHC and respond to peptide is most likely a direct consequence of enhanced surface expression per cell (see MFI values in Fig. 1B, 1C, Supplemental Fig. 1A). In contrast to wt TCR (38), TCR:28ε does not compete for endogenous CD3 proteins to become surface expressed, as evidenced by the lack of association between TCR:28ε and CD3ε (Figs. 3A, 5, Supplemental Fig. 2) and enhanced activation of NFAT when stimulating either TCR:28ε or the endogenous TCR in dual-TCR

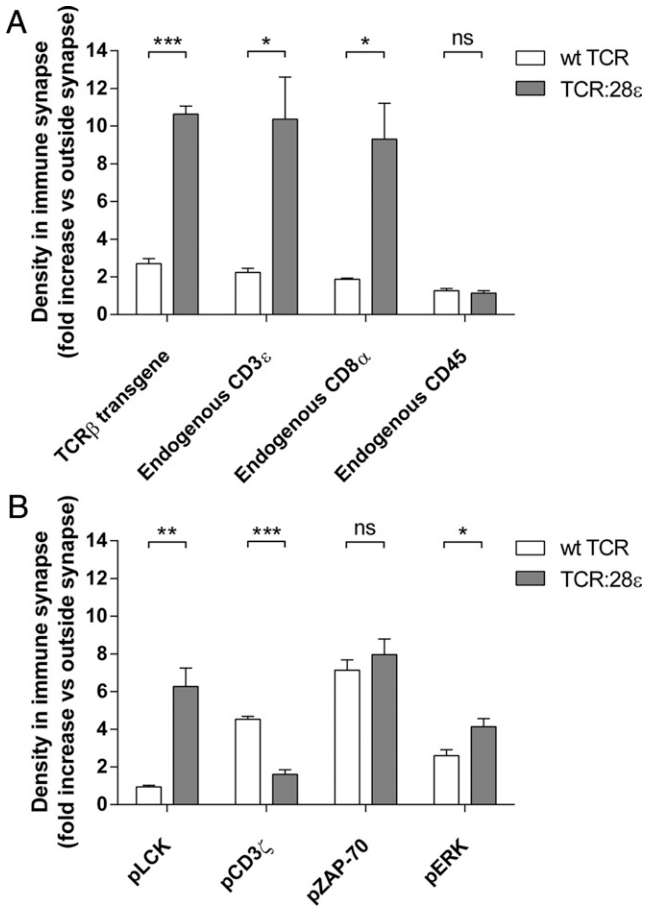

FIGURE 5. TCR:28ε T cells demonstrate enhanced synaptic accumulation of TCR, CD3ε, CD8α, p-LCK, and p-ERK. Jurkat T cells were transduced with M1/A1 wt TCR or TCR:28ε and sorted by FACS with TCRα and TCRβ mAbs, stimulated with APD B cells loaded with M1 peptide, and measured for densities of membrane (**A**) and IC (**B**) proteins in immune synapses. T cells were stained with TCR–Vβ9–PE mAb and one of the following mAbs (labeled with Alexa Fluor 647 or followed by isotype-specific GαM–Alexa Fluor 647): CD3ε, CD8α, CD45, p-CD3ζ, p-LCK, p-ERK, or p-ZAP70. T cells were analyzed by confocal microscopy. Data are densities of molecules (fold increase in signals inside versus outside immune synapses) + SEM ($n = 3$ independent measurements of 15 cells/measurement). TCR T cells stimulated with irrelevant peptide showed low background signals (data not shown). Data for wt TCR in (A) were modified from Roszik et al. (23). $*p < 0.05$, $**p < 0.005$, $***p < 0.0005$ TCR:28ε versus wt TCR, Student t test. ns, nonsignificant.

Jurkat T cells (Fig. 2A). Unexpectedly, T cell responses toward Ag^+ tumor cells were equal compared with wt TCR–transduced T cells. When testing TCR:28ε T cells in more detail, we observed a decreased effective dose of peptide yielding half-maximum response (Supplemental Fig. 4A), as well as a compromised response in the absence of CD8α binding (Supplemental Fig. 4B). These data, together with our observation that TCR:28ε does not show a decreased ability to associate with CD8α (Figs. 3A, 5A, Supplemental Fig. 2), suggest that TCR:28ε has a decreased affinity for peptide–MHC. The compromised peptide–MHC binding by TCR:28ε may be due to structural restraints of the fusion between TCR-C and the CD28 TM domains. Nevertheless, TCR:28ε enhances the strength of T cell responses at higher Ag concentrations (Supplemental Fig. 4A), which is most likely due to enhanced surface expression of TCR:28ε compared with wt TCR (Fig. 1B).

To dissect the contributions of TM and/or IC domains of CD28 and CD3ε to various TCR properties, we tested TCR:28ε variants and observed that CD28 TM domain affects surface TCR expression, whereas the combined actions of CD28 and CD3ε IC domains affect T cell functions (Fig. 4). The CD28 IC domain contains three main motifs that specifically associate with adaptor proteins and kinases, which, in turn, initiate different signal-transduction cascades (39). The proximal YMNM motif, when phosphorylated, binds p85 (a subunit of PI3K) and GRB2. The two distal proline-rich motifs bind ITK (PRRP motif) and GRB2, as well as FILAMIN-A and LCK (PYAPP motif). CD28 signal transduction via PI3K and GRB2 results in downstream activation of AKT and PLCγ1, respectively, which then results in activation of NF-κB and NFAT transcription factors and, consequently, T cell survival and IL-2 production. CD28 signal transduction via LCK feeds predominantly into the activation of NFAT and IL-2 production, most likely via enhanced stability of IL-2 mRNA and its secretion. In addition to the CD28 IC domain, the CD3ε IC domain binds GRK2 and CAST, which results in downstream activation of NFAT and IL-2 production (40, 41). The use of TCR variants either lacking or containing an LCK-nonbinding mutant of CD28 IC domain demonstrated a hierarchy with respect to dependency on CD28 signaling, in particular LCK signaling for different T cell functions (CD107a < IFN-γ < IL-2). This observed hierarchy is in line with an earlier report using a peptide–MHC ligand with compromised TCR binding (a partial agonist of the human $gp100_{280–288}$ peptide) (42). In fact, mobilization of CD107a generally requires limited T cell signaling and is presynthesized and ready to be mobilized, whereas production of cytokines requires de novo synthesis; in particular, IL-2 requires strong T cell signaling and NFAT activation.

TCR:28ε may be part of pre-existing clusters [as described for wt TCR/CD3 (43)] that are composed of dimers or oligomers of wt TCR/CD3 and TCR:28ε. The existence of such nanoclusters is suggested by the observed accumulation of endogenous TCR/CD3 complexes in immune synapses mediated by TCR:28ε (Fig. 6A). TCR/CD3 complexes may oligomerize via homotypic interactions governed by TCR-Cα and CD3ε (44, 45). According to such a model, TCR:28ε (encompassing TCR-Cα) and endogenous CD3ε are part of the same complex yet are interspersed with wt TCR and are not within 10 nm of each other (Figs. 3A, 5). We postulate that one important advantage of TCR:28ε over wt TCR is the formation of highly active immune synapses. Indeed, TCR:28ε-mediated, but not wt TCR-mediated, immune synapses were readily detectable in primary human T cells, showed enhanced accumulation of TCR, CD3, and CD8 (Figs. 5, 6), and are expected to facilitate Ag-dependent T cell activation (44, 46, 47). Notably, TCR:ζ mediates immune synapses in which densities of TCR, CD3, and CD8 are diluted over enlarged contact areas (23), whereas TCR:28ε mediates immune synapses in which densities of the aforementioned molecules are enriched in normal-sized immune synapses. We cannot exclude that TCR:28ε may differ from wt TCR with respect to its temporal organization of immune synapses. In fact, in primary human T cells we observed an association between the CD45 phosphatase and TCR:28ε, which may provide TCR:28ε with a kinetic advantage (Fig. 5B). In this respect, it is noteworthy that primary human T cells may require prolonged times to develop molecular clusters compared with Jurkat T cells (in which an association between CD45 and TCR:28ε was not observed) and may prove to be better suited for use in further experiments into the kinetics and stability of immune synapses (48, 49). Our results further argue that TCR:28ε facilitates the assembly of a molecular signaling scaffold at the immune synapse (Fig. 6). Enhanced densities of p-LCK within immune synapses may be a direct consequence of increased accumulations of TCR:28ε and CD8α, because both

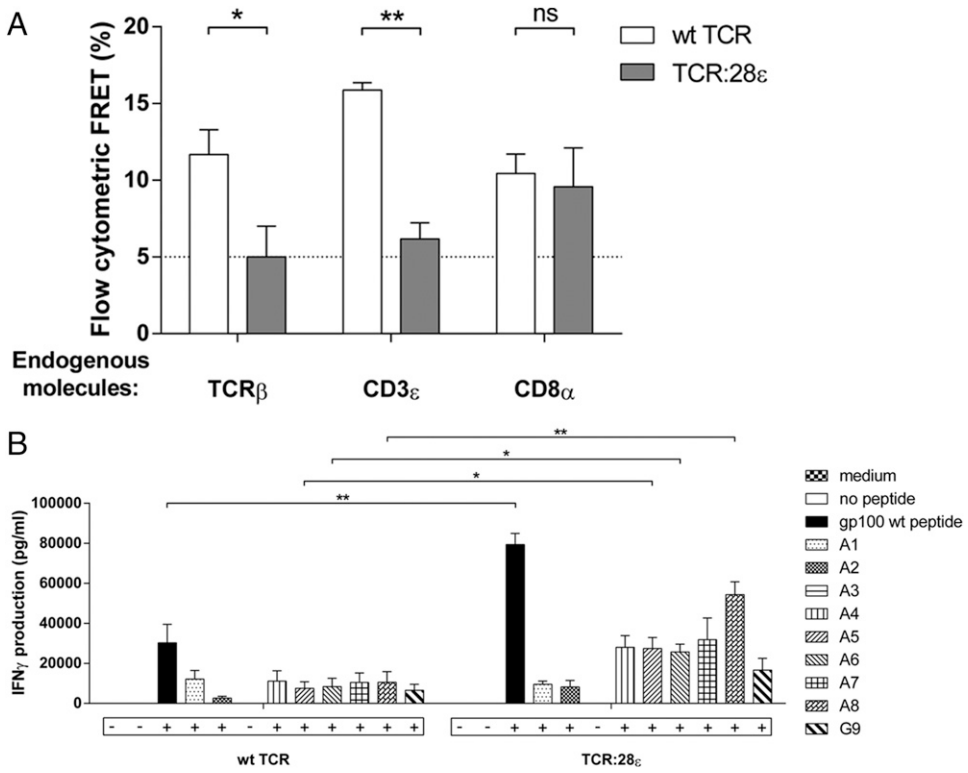

FIGURE 6. TCR:28ε does not appear prone to off-target reactivity in vitro. (**A**) Jurkat clone 19 T cells expressing MelanA/A2 TCR and CD8α were transduced with M1/A1 TCRs as described in the legend to Fig. 5. T cells were stained with the following three sets of Abs (1): TCR-Vα19 + RαM-Cy5 + TCR-Vβ27-PE (2); CD3ε + RαM-Cy5 + TCR-Vβ9-PE; and (3) CD8α + RαM-Cy5 + TCR-Vβ9-PE. Flow cytometry was used to measure Fluorescence Resonance Energy Transfer (FRET) and bars represent mean % + SEM, n = 3-6 independent measurements. Notably, FRET efficiencies below the dotted line representing a 5% background signal, do not imply that there is no pairing of molecules but do not allow distinction between significant and non-significant interactions. Mock T cells (no TCR transgene) showed negligible levels of FRET (data not shown). (**B**) TCR:28ε shows a peptide-fine specificity that is similar to that of wt TCR. Primary human T cells were transduced with empty virus particles or gp100/A2 TCRs as described in the legend to Fig. 2. T cells were O/N stimulated with T2 cells that were not loaded or loaded with gp100 wt peptide or altered peptide ligands (APL) (10^{-5} M final). APLs are coded by the letters A (Alanine) or G (Glycine) followed by a number that corresponds to the position of the amino acid that is altered into A or G in the gp100 wt peptide sequence (YLEPGPVTA). IFNγ production was measured by ELISA and expressed in pg/ml, n = 3 independent measurements. Notably, both wt TCR and TCR:28ε did not mediate a response to the A3 APL as indicated by "-", in contrast to other APLs as indicated by "+" (enhanced response compared with medium). Statistically significant differences between TCR:28ε and wt TCR were calculated with Student t test. *$p < 0.05$; **$p < 0.005$. ns, nonsignificant.

CD28 (contained in TCR:28ε) and CD8α harbor a motif for LCK recruitment. Activated ERK can phosphorylate LCK at serine 59, preventing inactivation of p-LCK by the phosphatase SHP-1 (50), thereby providing an alternative reason, and possibly a positive-feedback loop, for the enhanced activation of LCK. In TCR:28ε T cells, levels of p-CD3ζ were significantly lower compared with wt TCR T cells (Fig. 6B), which may be due to an inability of TCR:28ε to associate with endogenous CD3ζ and position this molecule sufficiently close to p-LCK to become phosphorylated. Despite the presence of fewer p-CD3ζ scaffolds, the accumulated levels of p-ZAP70 in TCR:28ε T cells were similar to those in wt TCR T cells (Fig. 6B), which may argue that ZAP70, even when docking to p-CD3ζ is hampered, becomes phosphorylated by the enhanced presence of p-LCK. The CD28 and CD3ε IC domains are able to contribute to the reorganization of the cytoskeleton and formation of immune synapses. The CD28 IC domain, mainly through its PYAPP motif and activation of GRB2 and FILAMIN-A pathways, directs movement of CD28 to early immune synapses (39), whereas the CD3ε IC domain, mainly through recruitment of NCK, leads to activation of the RAS/RAF/ERK pathway and formation of immune synapses (51, 52).

In addition to the ability of TCR:28ε to activate T cell responses, we investigated how sensitive this TCR is at mediating off-target reactivities. We observed that TCR:28ε does not mispair with endogenous TCR, as evidenced by flow cytometric FRET (Fig. 3A), nor does it have a changed peptide fine specificity compared with wt TCR (Fig. 3B), making this receptor less prone to induce off-target toxicities (9, 10). Interestingly, the 28ε cassette does not harbor the extracellular cysteine of CD28 (at position 141), which normally facilitates homodimerization of CD28 at the cell surface. However, this cysteine is not required per se for dimerization and costimulatory function (53). In addition to TCR mispairing and peptide fine specificity, our studies provide the following lines of evidence that TCR:28ε does not hamper safety by constitutively activating T cells: we did not observe activation of NFAT following nonspecific TCR stimulation (Fig. 2A); we did not observe CD107a mobilization or production of IFN-γ and IL-2 in the absence of Ag (Figs. 2B, 2C, 3B, Supplemental Fig. 1B, 1C); and TCR:28ε T cells revealed no enhanced proliferation during routine culture conditions (data not shown).

Finally, we assessed the in vivo behavior of T cells expressing TCR:28ε. HLA-A2–tg mice bearing an established B16 tumor expressing human gp100 and HLA-A2 were conditioned with busulphan and cyclophosphamide and treated with T cells transduced either with TCR:28ε or wt TCR. T cells expressing TCR:28ε effectively limited tumor recurrence (Fig. 7A) and delayed the time point at which tumors recurred following treatment (Fig. 7C). Notably, the effect on tumor recurrence was

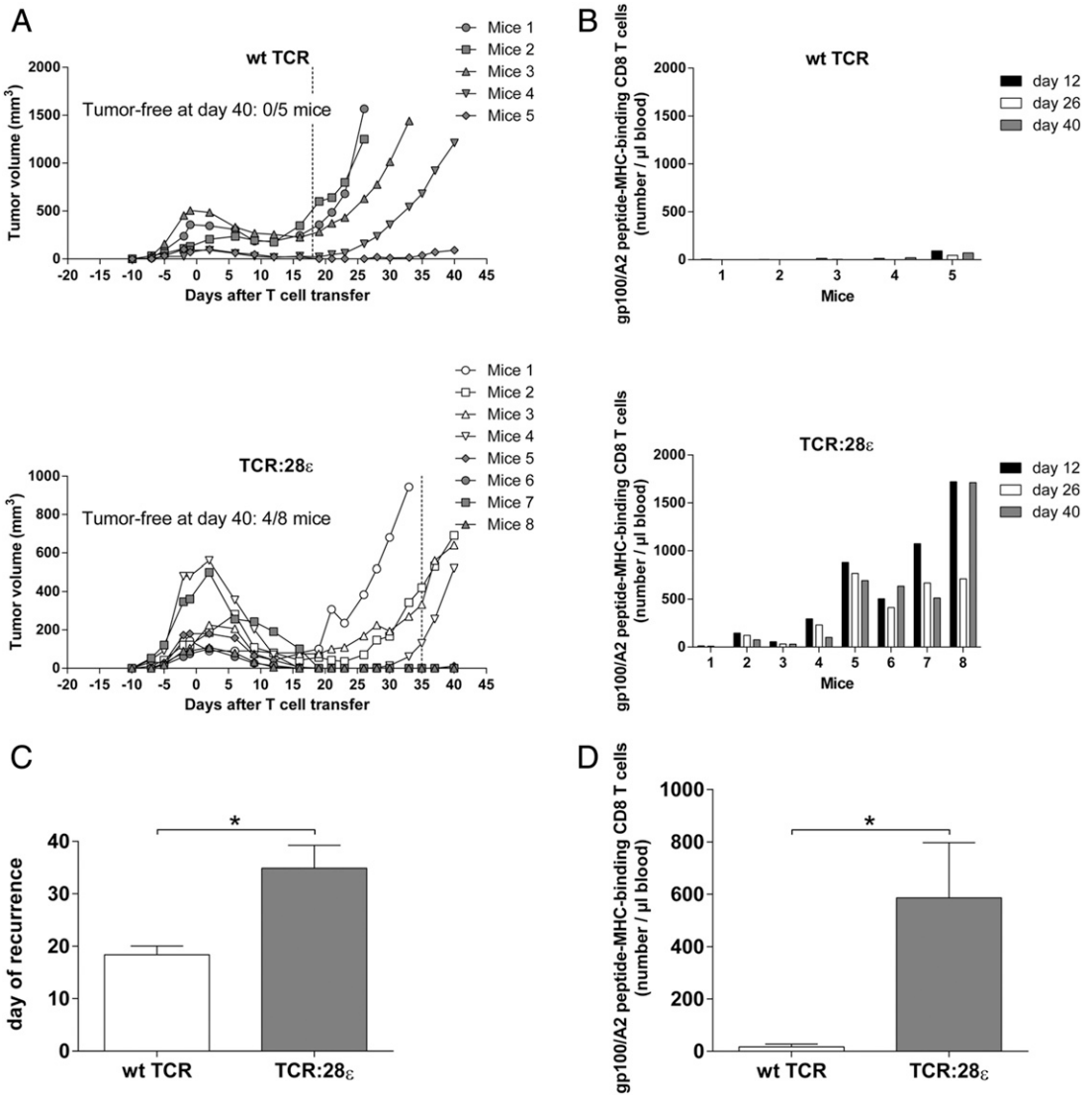

FIGURE 7. T cells expressing TCR:28ε decrease or delay tumor recurrence and enhance T cell persistence. (**A**) HLA-A2–tg mice were transplanted s.c. with B16:gp100/A2 cells at day 0. The tumor was left to grow for 10 d, after which mice received conditioning with busulphan and cyclophosphamide and injection of 7.5×10^6 T cells transduced either with TCR:28ε (*lower panel*) or wt TCR (*upper panel*). Tumor sizes were measured with a caliper and expressed as mm^3/individual mouse; mice that were tumor-free at day 40 are indicated and the mean day that tumors started to recur following treatment is indicated by the dotted line. (**B**) Peripheral blood was collected from mice at the indicated days following treatment with T cells transduced either with TCR:28ε (*lower panel*) or wt TCR (*upper panel*), and absolute numbers of peptide–MHC–binding CD8 T cells were determined by flow cytometry. Data are T cell numbers/individual mouse, with numbering of mice as shown in (A). (**C**) Tumor recurrences from (A) are presented as mean day + SEM. (**D**) T cell numbers from (B) are presented as mean + SEM. $*p < 0.05$ TCR:28ε versus wt TCR, Student *t* test.

accompanied by a drastic increase in the numbers of peripheral CD8 T cells that bound peptide–MHC (Fig. 7B, 7D). In fact, mice showing >400 peptide–MHC–binding CD8 T cells/μl blood appeared protected from tumor recurrence within 40 d posttreatment. T cells generally demonstrate early and preferential accumulation within Ag^+ tumors (54), but T cells appear to require sustained TCR- and CD28-mediated interactions to remain and accumulate in Ag^+ tissue (55). CD28 signaling enhances T cell survival, most likely through prevention of T cell apoptosis via inhibition of FasL (56) and stimulation of Bcl-x_L expression (57). These antiapoptotic pathways are most likely mediated through the CD28 motifs YMNM and PYAPP and binding of p85 and GRB2, with a dependence on NF-κB activation (39).

Most studies analyzing signaling cassettes were performed with CARs. Inclusion of CD28 into CARs, generally in combination with a CD3ζ domain, resulted in enhanced T cell activation and proliferation, in vivo T cell persistence, and antitumor effects. Signaling cassettes were tested further with other members of the CD28 family (58–62), such as CD137 (4-1BB) and CD134 (OX40), which showed promising results with respect to cytolysis, initiation or sustainment of an effective T cell response, and prevention of CAR-mediated proliferation of regulatory T cells (63). Importantly, clinical trials using CAR:CD28-CD3ζ or CAR:CD137-CD3ζ demonstrated significant objective responses in patients with B cell leukemia (16, 18, 19). In this study, we showed that a signaling cassette consisting of CD28 and CD3ε in the setting of TCRs improves the potency of T cell responses and peripheral T cell persistence without compromising Ag specificity and supports the further development of costimulatory TCRs for clinical testing.

Disclosures

The authors have no financial conflicts of interest.

References

1. Kunert, A., T. Straetemans, C. Govers, C. Lamers, R. Mathijssen, S. Sleijfer, and R. Debets. 2013. TCR-Engineered T Cells Meet New Challenges to Treat Solid Tumors: Choice of Antigen, T Cell Fitness, and Sensitization of Tumor Milieu. *Front. Immunol.* 4: 363.
2. Rosenberg, S. A. 2012. Raising the bar: the curative potential of human cancer immunotherapy. *Sci. Transl. Med.* 4: 127ps8.
3. Morgan, R. A., M. E. Dudley, J. R. Wunderlich, M. S. Hughes, J. C. Yang, R. M. Sherry, R. E. Royal, S. L. Topalian, U. S. Kammula, N. P. Restifo, et al. 2006. Cancer regression in patients after transfer of genetically engineered lymphocytes. *Science* 314: 126–129.
4. Robbins, P. F., R. A. Morgan, S. A. Feldman, J. C. Yang, R. M. Sherry, M. E. Dudley, J. R. Wunderlich, A. V. Nahvi, L. J. Helman, C. L. Mackall, et al. 2011. Tumor regression in patients with metastatic synovial cell sarcoma and melanoma using genetically engineered lymphocytes reactive with NY-ESO-1. *J. Clin. Oncol.* 29: 917–924.
5. Johnson, L. A., R. A. Morgan, M. E. Dudley, L. Cassard, J. C. Yang, M. S. Hughes, U. S. Kammula, R. E. Royal, R. M. Sherry, J. R. Wunderlich, et al. 2009. Gene therapy with human and mouse T-cell receptors mediates cancer regression and targets normal tissues expressing cognate antigen. *Blood* 114: 535–546.
6. Parkhurst, M. R., J. C. Yang, R. C. Langan, M. E. Dudley, D. A. Nathan, S. A. Feldman, J. L. Davis, R. A. Morgan, M. J. Merino, R. M. Sherry, et al. 2011. T cells targeting carcinoembryonic antigen can mediate regression of metastatic colorectal cancer but induce severe transient colitis. *Mol. Ther.* 19: 620–626.
7. Linette, G. P., E. A. Stadtmauer, M. V. Maus, A. P. Rapoport, B. L. Levine, L. Emery, L. Litzky, A. Bagg, B. M. Carreno, P. J. Cimino, et al. 2013. Cardiovascular toxicity and titin cross-reactivity of affinity-enhanced T cells in myeloma and melanoma. *Blood* 122: 863–871.
8. Morgan, R. A., N. Chinnasamy, D. Abate-Daga, A. Gros, P. F. Robbins, Z. Zheng, M. E. Dudley, S. A. Feldman, J. C. Yang, R. M. Sherry, et al. 2013. Cancer regression and neurological toxicity following anti-MAGE-A3 TCR gene therapy. *J. Immunother.* 36: 133–151.
9. van Loenen, M. M., R. de Boer, A. L. Amir, R. S. Hagedoorn, G. L. Volbeda, R. Willemze, J. J. van Rood, J. H. Falkenburg, and M. H. Heemskerk. 2010. Mixed T cell receptor dimers harbor potentially harmful neoreactivity. *Proc. Natl. Acad. Sci. USA* 107: 10972–10977.
10. Bendle, G. M., C. Linnemann, A. I. Hooijkaas, L. Bies, M. A. de Witte, A. Jorritsma, A. D. Kaiser, N. Pouw, R. Debets, E. Kieback, et al. 2010. Lethal graft-versus-host disease in mouse models of T cell receptor gene therapy. *Nat. Med.* 16: 565–570, 1p following 570.
11. Govers, C., Z. Sebestyén, M. Coccoris, R. A. Willemsen, and R. Debets. 2010. T cell receptor gene therapy: strategies for optimizing transgenic TCR pairing. *Trends Mol. Med.* 16: 77–87.
12. Provasi, E., P. Genovese, A. Lombardo, Z. Magnani, P. Q. Liu, A. Reik, V. Chu, D. E. Paschon, L. Zhang, J. Kuball, et al. 2012. Editing T cell specificity towards leukemia by zinc finger nucleases and lentiviral gene transfer. *Nat. Med.* 18: 807–815.
13. Besser, M. J., R. Shapira-Frommer, A. J. Treves, D. Zippel, O. Itzhaki, L. Hershkovitz, D. Levy, A. Kubi, E. Hovav, N. Chermoshniuk, et al. 2010. Clinical responses in a phase II study using adoptive transfer of short-term cultured tumor infiltration lymphocytes in metastatic melanoma patients. *Clin. Cancer Res.* 16: 2646–2655.
14. Dudley, M. E., J. R. Wunderlich, J. C. Yang, R. M. Sherry, S. L. Topalian, N. P. Restifo, R. E. Royal, U. Kammula, D. E. White, S. A. Mavroukakis, et al. 2005. Adoptive cell transfer therapy following non-myeloablative but lymphodepleting chemotherapy for the treatment of patients with refractory metastatic melanoma. *J. Clin. Oncol.* 23: 2346–2357.
15. Rosenberg, S. A., J. C. Yang, R. M. Sherry, U. S. Kammula, M. S. Hughes, G. Q. Phan, D. E. Citrin, N. P. Restifo, P. F. Robbins, J. R. Wunderlich, et al. 2011. Durable complete responses in heavily pretreated patients with metastatic melanoma using T-cell transfer immunotherapy. *Clin. Cancer Res.* 17: 4550–4557.
16. Kalos, M., B. L. Levine, D. L. Porter, S. Katz, S. A. Grupp, A. Bagg, and C. H. June. 2011. T cells with chimeric antigen receptors have potent antitumor effects and can establish memory in patients with advanced leukemia. *Sci. Transl. Med.* 3: 95ra73.
17. Couzin-Frankel, J. 2013. Breakthrough of the year 2013. Cancer immunotherapy. *Science* 342: 1432–1433.
18. Kochenderfer, J. N., M. E. Dudley, S. A. Feldman, W. H. Wilson, D. E. Spaner, I. Maric, M. Stetler-Stevenson, G. Q. Phan, M. S. Hughes, R. M. Sherry, et al. 2012. B-cell depletion and remissions of malignancy along with cytokine-associated toxicity in a clinical trial of anti-CD19 chimeric-antigen-receptor-transduced T cells. *Blood* 119: 2709–2720.
19. Brentjens, R. J., I. Rivière, J. H. Park, M. L. Davila, X. Wang, J. Stefanski, C. Taylor, R. Yeh, S. Bartido, O. Borquez-Ojeda, et al. 2011. Safety and persistence of adoptively transferred autologous CD19-targeted T cells in patients with relapsed or chemotherapy refractory B-cell leukemias. *Blood* 118: 4817–4828.
20. Butler, M. O., P. Friedlander, M. I. Milstein, M. M. Mooney, G. Metzler, A. P. Murray, M. Tanaka, A. Berezovskaya, O. Imataki, L. Drury, et al. 2011. Establishment of antitumor memory in humans using in vitro-educated CD8+ T cells. *Sci. Transl. Med.* 3: 80ra34.
21. Van de Griend, R. J., B. A. Van Krimpen, S. J. Bol, A. Thompson, and R. L. Bolhuis. 1984. Rapid expansion of human cytotoxic T cell clones: growth promotion by a heat-labile serum component and by various types of feeder cells. *J. Immunol. Methods* 66: 285–298.
22. Sebestyén, Z., E. Schooten, T. Sals, I. Zaldivar, E. San José, B. Alarcón, S. Bobisse, A. Rosato, J. Szöllosi, J. W. Gratama, et al. 2008. Human TCR that incorporate CD3zeta induce highly preferred pairing between TCRalpha and beta chains following gene transfer. *J. Immunol.* 180: 7736–7746.
23. Roszik, J., Z. Sebestyén, C. Govers, Y. Guri, A. Szöor, Z. Pályi-Krekk, G. Vereb, P. Nagy, J. Szöllosi, and R. Debets. 2011. T-cell synapse formation depends on antigen recognition but not CD3 interaction: studies with TCR:ζ, a candidate transgene for TCR gene therapy. *Eur. J. Immunol.* 41: 1288–1297.
24. Govers, C., C. Berrevoets, E. Treffers-Westerlaken, M. Broertjes, and R. Debets. 2012. Magnetic-activated cell sorting of TCR-engineered T cells, using tCD34 as a gene marker, but not peptide-MHC multimers, results in significant numbers of functional CD4(+) and CD8(+) T cells. *Human Gene Ther. Meth.* 23: 213–224.
25. Schaft, N., R. A. Willemsen, J. de Vries, B. Lankiewicz, B. W. Essers, J. W. Gratama, C. G. Figdor, R. L. Bolhuis, R. Debets, and G. J. Adema. 2003. Peptide fine specificity of anti-glycoprotein 100 CTL is preserved following transfer of engineered TCR alpha beta genes into primary human T lymphocytes. *J. Immunol.* 170: 2186–2194.
26. van der Bruggen, P., C. Traversari, P. Chomez, C. Lurquin, E. De Plaen, B. Van den Eynde, A. Knuth, and T. Boon. 1991. A gene encoding an antigen recognized by cytolytic T lymphocytes on a human melanoma. *Science* 254: 1643–1647.
27. Willemsen, R. A., M. E. Weijtens, C. Ronteltap, Z. Eshhar, J. W. Gratama, P. Chames, and R. L. Bolhuis. 2000. Grafting primary human T lymphocytes with cancer-specific chimeric single chain and two chain TCR. *Gene Ther.* 7: 1369–1377.
28. Schaft, N., B. Lankiewicz, J. Drexhage, C. Berrevoets, D. J. Moss, V. Levitsky, M. Bonneville, S. P. Lee, A. J. McMichael, J. W. Gratama, et al. 2006. T cell retargeting to EBV antigens following TCR gene transfer: CD28-containing receptors mediate enhanced antigen-specific IFNgamma production. *Int. Immunol.* 18: 591–601.
29. Kofler, D. M., M. Chmielewski, G. Rappl, A. Hombach, T. Riet, A. Schmidt, A. A. Hombach, C. M. Wendtner, and H. Abken. 2011. CD28 costimulation impairs the efficacy of a redirected T-cell antitumor attack in the presence of regulatory T cells which can be overcome by preventing Lck activation. *Mol. Ther.* 19: 760–767.
30. Lamers, C. H., R. A. Willemsen, P. van Elzakker, B. A. van Krimpen, J. W. Gratama, and R. Debets. 2006. Phoenix-ampho outperforms PG13 as retroviral packaging cells to transduce human T cells with tumor-specific receptors: implications for clinical immunogene therapy of cancer. *Cancer Gene Ther.* 13: 503–509.
31. Govers, C., Z. Sebestyen, C. Berrevoets, H. Venselaar, and R. Debets. 2011. T cell receptor fused to CD3ζ: transmembrane domain of CD3ζ prevents TCR mis-pairing, whereas complete CD3ζ directs functional TCR expression. *Open Gene Ther. J.* 4: 11–22.
32. Roszik, J., J. Szöllosi, and G. Vereb. 2008. AccPbFRET: an ImageJ plugin for semi-automatic, fully corrected analysis of acceptor photobleaching FRET images. *BMC Bioinformatics* 9: 346.
33. Szentesi, G., G. Horváth, I. Bori, G. Vámosi, J. Szöllosi, R. Gáspár, S. Damjanovich, A. Jenei, and L. Mátyus. 2004. Computer program for determining fluorescence resonance energy transfer efficiency from flow cytometric data on a cell-by-cell basis. *Comput. Methods Programs Biomed.* 75: 201–211.
34. Pascolo, S., N. Bervas, J. M. Ure, A. G. Smith, F. A. Lemonnier, and B. Pérarnau. 1997. HLA-A2.1-restricted education and cytolytic activity of CD8 (+) T lymphocytes from beta2 microglobulin (beta2m) HLA-A2.1 monochain transgenic H-2Db beta2m double knockout mice. *J. Exp. Med.* 185: 2043–2051.
35. Pouw, N. M., E. J. Westerlaken, R. A. Willemsen, and R. Debets. 2007. Gene transfer of human TCR in primary murine T cells is improved by pseudo-typing with amphotropic and ecotropic envelopes. *J. Gene Med.* 9: 561–570.
36. Seynhaeve, A. L., S. Hoving, D. Schipper, C. E. Vermeulen, Ga. de Wiel-Ambagtsheer, S. T. van Tiel, A. M. Eggermont, and T. L. Ten Hagen. 2007. Tumor necrosis factor alpha mediates homogeneous distribution of liposomes in murine melanoma that contributes to a better tumor response. *Cancer Res.* 67: 9455–9462.
37. Wooldridge, L., H. A. van den Berg, M. Glick, E. Gostick, B. Laugel, S. L. Hutchinson, A. Milicic, J. M. Brenchley, D. C. Douek, D. A. Price, and A. K. Sewell. 2005. Interaction between the CD8 coreceptor and major histocompatibility complex class I stabilizes T cell receptor-antigen complexes at the cell surface. *J. Biol. Chem.* 280: 27491–27501.
38. Sussman, J. J., J. S. Bonifacino, J. Lippincott-Schwartz, A. M. Weissman, T. Saito, R. D. Klausner, and J. D. Ashwell. 1988. Failure to synthesize the T cell CD3-zeta chain: structure and function of a partial T cell receptor complex. *Cell* 52: 85–95.
39. Boomer, J. S., and J. M. Green. 2010. An enigmatic tail of CD28 signaling. *Cold Spring Harb. Perspect. Biol.* 2: a002436.
40. Gallo, E. M., K. Canté-Barrett, and G. R. Crabtree. 2006. Lymphocyte calcium signaling from membrane to nucleus. *Nat. Immunol.* 7: 25–32.
41. DeFord-Watts, L. M., J. A. Young, L. A. Pitcher, and N. S. van Oers. 2007. The membrane-proximal portion of CD3 epsilon associates with the serine/threonine kinase GRK2. *J. Biol. Chem.* 282: 16126–16134.
42. Schaft, N., M. Coccoris, J. Drexhage, C. Knoop, I. J. de Vries, G. J. Adema, and R. Debets. 2013. An Altered gp100 Peptide Ligand with Decreased Binding by TCR and CD8α Dissects T Cell Cytotoxicity from Production of Cytokines and Activation of NFAT. *Front. Immunol.* 4: 270.
43. Blanco, R., and B. Alarcón. 2012. TCR Nanoclusters as the Framework for Transmission of Conformational Changes and Cooperativity. *Front. Immunol.* 3: 115.
44. Kuhns, M. S., A. T. Girvin, L. O. Klein, R. Chen, K. D. Jensen, E. W. Newell, J. B. Huppa, B. F. Lillemeier, M. Huse, Y. H. Chien, et al. 2010. Evidence for

a functional sidedness to the alphabetaTCR. *Proc. Natl. Acad. Sci. USA* 107: 5094–5099.
45. Kumar, R., M. Ferez, M. Swamy, I. Arechaga, M. T. Rejas, J. M. Valpuesta, W. W. Schamel, B. Alarcon, and H. M. van Santen. 2011. Increased sensitivity of antigen-experienced T cells through the enrichment of oligomeric T cell receptor complexes. *Immunity* 35: 375–387.
46. Fernández-Miguel, G., B. Alarcón, A. Iglesias, H. Bluethmann, M. Alvarez-Mon, E. Sanz, and A. de la Hera. 1999. Multivalent structure of an alphabetaT cell receptor. *Proc. Natl. Acad. Sci. USA* 96: 1547–1552.
47. Schamel, W. W., I. Arechaga, R. M. Risueño, H. M. van Santen, P. Cabezas, C. Risco, J. M. Valpuesta, and B. Alarcón. 2005. Coexistence of multivalent and monovalent TCRs explains high sensitivity and wide range of response. *J. Exp. Med.* 202: 493–503.
48. Ahmed, F., S. Friend, T. C. George, N. Barteneva, and J. Lieberman. 2009. Numbers matter: quantitative and dynamic analysis of the formation of an immunological synapse using imaging flow cytometry. *J. Immunol. Methods* 347: 79–86.
49. Bunnell, S. C., D. I. Hong, J. R. Kardon, T. Yamazaki, C. J. McGlade, V. A. Barr, and L. E. Samelson. 2002. T cell receptor ligation induces the formation of dynamically regulated signaling assemblies. *J. Cell Biol.* 158: 1263–1275.
50. Stefanová, I., B. Hemmer, M. Vergelli, R. Martin, W. E. Biddison, and R. N. Germain. 2003. TCR ligand discrimination is enforced by competing ERK positive and SHP-1 negative feedback pathways. *Nat. Immunol.* 4: 248–254.
51. Schneider, H., and C. E. Rudd. 2008. CD28 and Grb-2, relative to Gads or Grap, preferentially co-operate with Vav1 in the activation of NFAT/AP-1 transcription. *Biochem. Biophys. Res. Commun.* 369: 616–621.
52. Lin, J., and A. Weiss. 2001. T cell receptor signalling. *J. Cell Sci.* 114: 243–244.
53. Lazar-Molnar, E., S. C. Almo, and S. G. Nathenson. 2006. The interchain disulfide linkage is not a prerequisite but enhances CD28 costimulatory function. *Cell. Immunol.* 244: 125–129.
54. Charo, J., C. Perez, C. Buschow, A. Jukica, M. Czeh, and T. Blankenstein. 2011. Visualizing the dynamic of adoptively transferred T cells during the rejection of large established tumors. *Eur. J. Immunol.* 41: 3187–3197.
55. David, R., L. Ma, A. Ivetic, A. Takesono, A. J. Ridley, J. G. Chai, V. L. Tybulewicz, and F. M. Marelli-Berg. 2009. T-cell receptor- and CD28-induced Vav1 activity is required for the accumulation of primed T cells into antigenic tissue. *Blood* 113: 3696–3705.
56. Kirchhoff, S., W. W. Müller, M. Li-Weber, and P. H. Krammer. 2000. Up-regulation of c-FLIPshort and reduction of activation-induced cell death in CD28-costimulated human T cells. *Eur. J. Immunol.* 30: 2765–2774.
57. Boise, L. H., A. J. Minn, P. J. Noel, C. H. June, M. A. Accavitti, T. Lindsten, and C. B. Thompson. 1995. CD28 costimulation can promote T cell survival by enhancing the expression of Bcl-XL. *Immunity* 3: 87–98.
58. Zhao, Y., Q. J. Wang, S. Yang, J. N. Kochenderfer, Z. Zheng, X. Zhong, M. Sadelain, Z. Eshhar, S. A. Rosenberg, and R. A. Morgan. 2009. A herceptin-based chimeric antigen receptor with modified signaling domains leads to enhanced survival of transduced T lymphocytes and antitumor activity. *J. Immunol.* 183: 5563–5574.
59. Tammana, S., X. Huang, M. Wong, M. C. Milone, L. Ma, B. L. Levine, C. H. June, J. E. Wagner, B. R. Blazar, and X. Zhou. 2010. 4-1BB and CD28 signaling plays a synergistic role in redirecting umbilical cord blood T cells against B-cell malignancies. *Hum. Gene Ther.* 21: 75–86.
60. Pule, M. A., K. C. Straathof, G. Dotti, H. E. Heslop, C. M. Rooney, and M. K. Brenner. 2005. A chimeric T cell antigen receptor that augments cytokine release and supports clonal expansion of primary human T cells. *Mol. Ther.* 12: 933–941.
61. Milone, M. C., J. D. Fish, C. Carpenito, R. G. Carroll, G. K. Binder, D. Teachey, M. Samanta, M. Lakhal, B. Gloss, G. Danet-Desnoyers, et al. 2009. Chimeric receptors containing CD137 signal transduction domains mediate enhanced survival of T cells and increased antileukemic efficacy in vivo. *Mol. Ther.* 17: 1453–1464.
62. Carpenito, C., M. C. Milone, R. Hassan, J. C. Simonet, M. Lakhal, M. M. Suhoski, A. Varela-Rohena, K. M. Haines, D. F. Heitjan, S. M. Albelda, et al. 2009. Control of large, established tumor xenografts with genetically retargeted human T cells containing CD28 and CD137 domains. *Proc. Natl. Acad. Sci. USA* 106: 3360–3365.
63. Gilham, D. E., R. Debets, M. Pule, R. E. Hawkins, and H. Abken. 2012. CAR-T cells and solid tumors: tuning T cells to challenge an inveterate foe. *Trends Mol. Med.* 18: 377–384.